Processing and Application of Ceramics 18 [1] (2024) 98–108
https://doi.org/10.2298/PAC2401098P

Influence of the second metal component on processing and selected properties of Al_2O_3-Cu hybrid composites

Paulina Piotrkiewicz[1], Justyna Zygmuntowicz[1,*], Marcin Wachowski[2], Ireneusz Szachogłuchowicz[2], Waldemar Kaszuwara[1]

[1]*Warsaw University of Technology, Faculty of Materials Science and Engineering, 141 Woloska Str., 02-507 Warsaw, Poland*
[2]*Military University of Technology, Faculty of Mechanical Engineering, gen. S. Kaliskiego 2 St., 00-908 Warsaw, Poland*

Received 20 September 2023; Received in revised form 26 February 2024; Accepted 17 March 2024

Abstract

The aim of the work was to determine the influence of metallic phase content on the obtained properties of hybrid composites from the ceramics-metal system. Six series of samples from three systems (Al_2O_3-Cu, Al_2O_3-Cu-Ni and Al_2O_3-Cu-Cr) with two different contents of metallic phase (2.5 and 10 vol.%) were prepared by uniaxial pressing and pressure-less sintering. The research carried out in this work used the classic idea of material engineering, assuming the optimization of the material's functional properties by shaping the microstructure in a suitably modified technological process. The possibility of producing composite samples with density exceeding 95 %TD was confirmed. There was no significant effect of the composition and the share of the metallic phase on the obtained values. The microstructure observations showed that the addition of the second metallic component had a positive effect on the size of the metallic particles, limiting the formation of metal clusters of significant size visible in the case of Al_2O_3-Cu samples. Compressive strength tests have shown that the addition of the second component to the metallic phase has a positive effect on the compressive strength of the material.

Keywords: *alumina-copper composites, pressing, mechanical properties, structural characterization*

I. Introduction

The constantly developing technology forces continuos processes of improvement and development of new materials. Composites, as a group of materials combining the properties of components with completely different characteristics at first glance, provide one of the solutions to meet modern technological challenges. Among the various groups of composite materials, ceramics-metal composites are one of the widely described in the literature with great potential for development. There are many reports on the positive effect of adding metal to the ceramic matrix. This impact is considered both in the context of improving the mechanical properties of ceramics, as well as the possibility of introducing completely new properties to the material through the appropriate metallic component. At the same time, the obtained material retains the most important features characterizing its ceramic matrix, such as high hardness or resistance to thermal shocks [1]. Due to these possibilities, the variety of applications for this group of materials, ranging from aviation, through the automotive and defence industries, to biomedical applications [2] is not surprising.

Al_2O_3-metal based composites are the most popular ceramics-metal system. Corundum is a material with high availability, having a set of beneficial features such as low weight, high hardness, resistance to thermal shocks and aggressive chemicals, high corrosion resistance, biocompatibility [3,4]. The main disadvantage, constituting an obstacle to the use of alumina ceramics in areas requiring specific mechanical properties, is its low fracture toughness and, consequently, the tendency to develop cracks in an uncontrolled manner [3,4]. The solution to this problem is sought in the use of a metal

* Corresponding author: tel: +48 22 2348138
e-mail: *Justyna.zygmuntowicz@pw.edu.pl*

addition to the Al_2O_3 ceramic matrix. Studies show that the combination of hard but brittle ceramics with supple, soft metal leads to the creation of a material with completely new possibilities [5,6]. Analysing the available literature on the subject, it can be seen that the incorporation of metals, such as: Ag [7], Ti [8], Ni [9], Al [10] or Cr [11] into the ceramic matrix is successfully implemented and contributes to significant improvement in mechanical properties compared to pure ceramics. Among the metals used, a lot of attention is also given to Cu as it has excellent thermal and electrical conductivity [12]. The combination of these features with the strength of ceramics brings great opportunities for applications in various areas of industry, previously unavailable for materials based on ceramics. However, the low melting temperature of Cu (T_{Cu} = 1084 °C [13]) is a major obstacle in the process of forming composites from this system. The copper melting process takes place at a temperature below the standard sintering temperatures for alumina ceramics. For this reason, the sintering process of Al_2O_3-Cu composites is sintering in the presence of liquid phase. In combination with poor adhesion of Cu to Al_2O_3 [14], this creates the risk of metal evaporation from the sample during the forming process, which in turn may have an adverse effect on the properties of the obtained material.

Many different solutions are used to produce Al_2O_3-Cu based composite with good density and mechanical properties. The problem of poor adhesion between copper and Al_2O_3 can be solved, for example, by using copper oxide or copper nitride instead of pure metal as the starting material in the composite forming process [15]. Another possibility is by applying a layer of another metal improving the adhesive properties to copper on the surface of ceramic particles (for example by covering Al_2O_3 particles with a layer of nickel) [16]. In the case of Al_2O_3-Cu composites produced by the infiltration method, increased pressure is used to improve the adhesion between the components [17], but also the activation of ceramic preform with a layer of reactive metal, e.g. Ti [18] or hot pressing of the metal powder filling the ceramic preform prepared in a separate process [19]. One of the solutions used is also the production of Al_2O_3-Cu composites by processes that combine simultaneous moulding and sintering, such as hot pressing [20] or processes based on high-current sintering, such as SPS [21,22] or PECS [23]. This makes it possible to shorten the sintering time and possibly lower the process temperature without compromising the mechanical properties. However, these processes are more complicated than in the case of conventional methods and require higher financial outlays. On the other hand, there are studies confirming the possibility of producing Al_2O_3-Cu composites by conventional methods, e.g. by uniaxial pressing [24,25], or slip casting, according to the work of Stratigaki *et al.* [26].

Another approach to the topic of producing composites based on Al_2O_3 with Cu is the addition of a second metallic component. Its main purpose is to retain Cu within the sample during the sintering process. Earlier work carried out in our team showed that it is possible to produce Al_2O_3-Cu-Cr [27] and Al_2O_3-Cu-Ni [28–30] composites characterized by good densification and mechanical properties. In the case of composites from the Al_2O_3-Cu-Cr system, tests have shown that chromium does not react with liquid copper during the sintering process. However, the physical presence of solid particles of the second metal characterized by good adhesion to Cu causes that liquid copper during the sintering process surrounds chromium particles located in the ceramic matrix and is physically retained by them inside the sample. Studies have also confirmed that Cr improves the mechanical resistance of the composite [27]. In the case of composites from the Al_2O_3-Cu-Ni system, according to the equilibrium system for these metals [31], copper at the sintering temperature can react with nickel to form a CuNi solid solution [28–30]. The emerging new phase binds part of the liquid copper present in the structure. Characterized by a melting point higher than pure copper (1170–1240 °C [32,33]), it allows the Al_2O_3 particles to close the copper within the matrix during sintering and, consequently, limits its evaporation to the surface of the sample [28,29]. It was also confirmed that the presence of Ni had a positive effect on the mechanical properties of the produced composites, which achieved higher hardness than the Al_2O_3-Cu samples produced by the analogous method, without compromising their fracture toughness [28]. However, in the case of composites with Cr or Ni as the second metallic component, their effect on improving the adhesion between the matrix and the metallic phase were not found [27–30].

This article analyses the possibility of producing Al_2O_3-Cu based composites, and how the forming process and the properties of the final material are affected by the addition of a second metal (Cr or Ni) to the metallic phase. Samples from the three systems Al_2O_3-Cu, Al_2O_3-Cu-Ni and Al_2O_3-Cu-Cr were prepared from the starting powders by uniaxial pressing followed by the pressure-less sintering. In order to determine the influence of the content of the metallic phase on the obtained properties of the composites, samples containing 2.5 and 10 vol.% of the metallic phase were produced.

II. Experimental

2.1. Sample preparation

The forming process was multi-stage and starting materials were Al_2O_3 powder (TM-DAR, 120 nm, 99.99% purity) and metallic powders: Cu (Createc, <150 μm, 99.98% purity), Ni (Createc, <50 μm, 99.98% purity) and Cr (Createc, 3–7 μm, 99.98% purity). In the first stage, powder mixtures from three systems (Al_2O_3-Cu, Al_2O_3-Cu-Ni and Al_2O_3-Cu-Cr) were prepared from the starting powders. For this purpose, the starting powders were weighed in appropriate proportions

and subjected to homogenization in the Retsch PM400 planetary-ball mill for 1 h at a rate of 300 rpm in the presence of a liquid medium (ethanol). Then, the obtained masses were dried in a laboratory drier at 30 °C for 24 h until complete evaporation of alcohol. After drying, the masses were subjected to granulation using sieves with a gradation of 600, 400 and 150 μm, respectively. The powder mixtures prepared in this way were then combined with a binder and re-granulated on sieves of the same gradation.

In the second stage the powder masses were formed into solid shapes using a hydraulic press in a cemented carbide matrix with a diameter of $\varnothing = 20$ mm, at a pressing pressure of 100 MPa. A 10% solution of polyvinyl alcohol (PVA) in the amount of 10% of the total weight of the powders was used as a binder. The raw mouldings obtained as a result of the pressing process were then sintered in a tube furnace at 1400 °C for 2 h in the third stage. The sintering process for each system was carried out separately and in a reducing atmosphere (5%H_2/95%Ar) in order to limit the oxidation of metallic components and the formation of spinels.

In this way, six composite samples were produced from three systems: Al_2O_3-Cu, Al_2O_3-Cu-Ni and Al_2O_3-Cu-Cr. The samples within one system had different content of the metallic phase equal to 2.5 or 10 vol.%. In the case of three-component systems, the volume fraction of both components of the metallic phase (Cu and Ni/Cr) was the same. Table 1 lists the designations of individual series along with their basic characteristics.

2.2. Sample characterization

In the first stage of the research, the powders used to produce the composites were characterized. For this purpose, the phase composition, microstructure and density of the powders were analysed. Microscopic observations of the powders were made using the JSM-6610 scanning electron microscope. The powders were viewed in the secondary electrons mode at 15 kV. The study of the phase composition of the powders was carried out by X-ray diffraction method on Rigaku Mini Flex II (Japan) diffractometer. The source of radiation was an X-ray tube with a copper anode with a wavelength of the Kα radiation line of $\lambda = 1.54178$ Å. The test was carried out in the angular range of 2θ: 20–100° with a 0.01° step, using the current of 15 mA and the voltage of 30 kV. The diffraction signal counting time was 1 s. The obtained XRD patterns were analysed using the PDF+4 2022 standard database and the Jade 8.5 (Materials Data) program correlated with it. The density of the powders was measured using an AccuPyc 1340 II helium pycnometer from Micrometrics (USA). The measurements were carried out using He by using the filling pressure of the measuring cell of 1.3 bar. The measurement consisted of a sequence of 10 purges and 700 cycles.

The obtained composite samples after sintering process were subjected to macroscopic and microscopic observations. For this purpose, the surfaces of the fabricated specimens were processed by grinding on diamond discs and by polishing. After preparation the surfaces of the produced sinters were subjected to observations using the Olympus LEXT OLS4100 confocal microscope in order to make a general assessment of the metallic phase distribution in the composite structure. Density of the sintered samples was determined using the Archimedes method. X-ray diffraction (XRD) measurements were carried out to determine the phase composition and possible phase transformations occurring during the sintering process in the produced composites. The tests were carried out with analogous parameters as for the starting powders.

Compression tests were carried out using an Instron 8802MT hydraulic pulsator for inducing monotonic loads with a worktable for the implementation of complex states of stress. The pulsator is designed to generate loads up to 250 kN. The tests were carried out at room temperature. Digital image correlation studies were carried out using the Dantec Dynamics Q-400 DIC device. This method allows to present a map of deformations and displacements in the tested element without contact. Istra 4.7D software was used for data analysis.

The fractures of the produced samples after the sintering process were observed on the JEOL JSM-6610 scanning electron microscope. Ceramics require thermal etching to reveal grain boundaries. Due to the low melting temperature of copper (1084 °C), close to the standard etching temperature, the use of this process would involve a change in the structure of the samples during the process, as well as the risk of their degradation due to the outflow of copper outside the sample area. For this reason, it was decided to use the observations of fractured surface of the samples. The detection of Al_2O_3 grains was carried out manually, taking into account the fracture structure. The obtained contours of

Table 1. Comparison of ST-4 proppant properties with other products, such as: sand, low-density ceramic proppants produced by Wu *et al.* [58], low-density ceramic proppants from Carbo Company and the required value of Chinese petroleum and natural gas industry standards (SY/T5108-2014) for low-density proppants

Sample	Composition	Content of the metallic phase	Sintering conditions
A-Cu(2.5)	Al2O3-Cu	2.5 vol.%	
A-Cu(10)	Al2O3-Cu	10 vol.%	
A-Cu-Ni(2.5)	Al2O3-Cu-Ni	2.5 vol.% (50 wt.% Cu : 50 wt.% Ni)	1400 °C, reducing
A-Cu-Ni(10)	Al2O3-Cu-Ni	10 vol.% (50 wt.% Cu : 50 wt.% Ni)	atmosphere: Ar/H_2
A-Cu-Cr(2.5)	Al2O3-Cu-Cr	2.5 vol.% (50 wt.% Cu : 50 wt.% Cr)	
A-Cu-Cr(10)	Al2O3-Cu-Cr	10 vol.% (50 wt.% Cu : 50 wt.% Ni)	

the ceramic matrix grains were subjected to appropriate image modifications, and the resulting binary image was analysed using the Micrometer software. On the basis of the obtained results, the value of the average equivalent diameter d_2 was determined for each of the produced series and histograms showing the percentage distribution of the value of the average equivalent diameter were made. In addition, in the next stage of the research, shape parameters for Al_2O_3 grains were determined.

III. Results and discussion

Figure 1 presents the results of microscopic observations of the starting powders. The alumina ceramic powder was characterized by a uniaxial morphology, with a tendency to form larger agglomerates. The Ni powder has a granular shape of particles of various sizes, similarly to the ceramic powder with a tendency to form agglomerates. The Cu powder has a dendritic particle shape, while the Cr powder showed a polyhedral morphology with a clear division into fractions with different sizes of individual particles. In the case of Cu and Cr powders, no tendency to agglomeration was observed (PN-EN ISO 3252:2019-12).

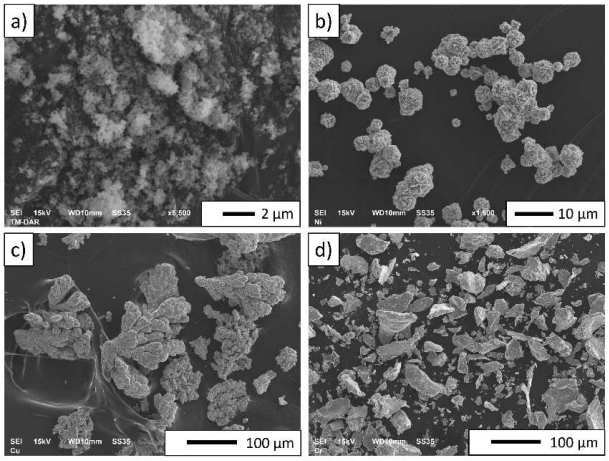

Figure 1. Micrographs of the starting powders: a) Al_2O_3, b) nickel, c) copper and d) chromium

The phase composition analysis of the initial powders used in the moulding process (Fig. 2) confirmed their single-phase structure. The presence of reflections characteristics of α-Al_2O_3 (PDF #98-000-0174) was confirmed (Fig. 2a). On the other hand, in metallic powders, the reflections visible in the diffractograms confirmed the presence of nickel (Fig. 2b; PDF #04-003-7263), copper (Fig. 2c; PDF #04-003-5318) and chromium (Fig 2d; PDF #04-025-0975).

The actual densities of the starting Al_2O_3, Cu, Ni and Cr powders, measured using a helium pycnometer, were equal to 3.99 ± 0.03, 8.96 ± 0.02, 8.9 ± 0.02 and 7.03 ± 0.02 g/cm^3, respectively. The measured values are close to their theoretical density, which also confirms high purity of the used materials.

Observations of the samples' surface after sintering, made with the use of a confocal microscope (Fig. 3), allowed to conclude that the metallic particles in the ceramic matrix of the composite are distributed randomly, but evenly. In the case of the samples with copper (Fig. 3a), metal particles remaining in the liquid phase during the sintering process merged into larger clusters, visible in the photos of the series A-Cu(2.5) and A-Cu(10). The samples from the three-component systems: Al_2O_3-Cu-Ni (Fig. 3b) and Al_2O_3-Cu-Cr (Fig. 3c) were characterized by a significantly lower content of large metallic particles in the matrix, both in the case of the samples with 2.5 vol.% (series A-Cu-Ni(2.5), A-Cu-Cr(2.5)) as well as 10 vol.% of the metallic phase content (series A-Cu-Cr(2.5), A-Cu-Cr(10)). In addition, the presence of porosity was found on the surfaces of the observed samples.

There was no significant effect of the metallic phase content on the relative density. All produced samples were characterized by a similar relative density at the

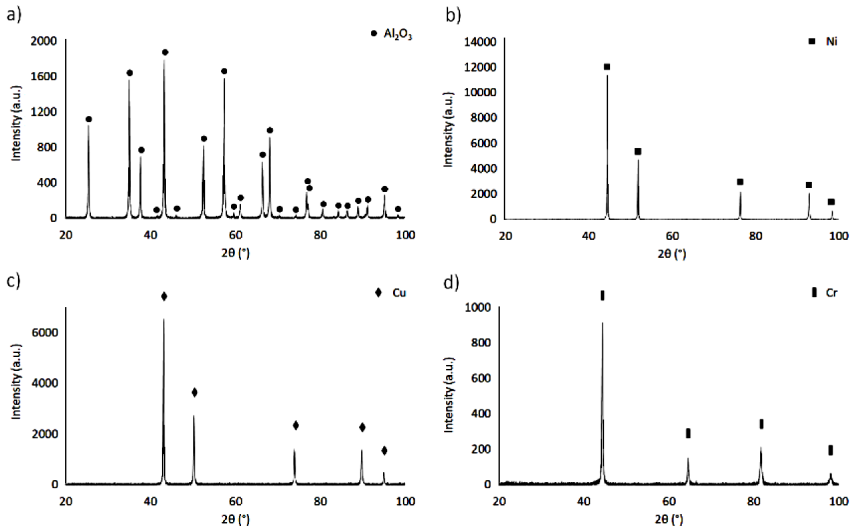

Figure 2. XRD patterns of the starting powders: a) aluminium oxide, b) nickel, c) copper and d) chromium

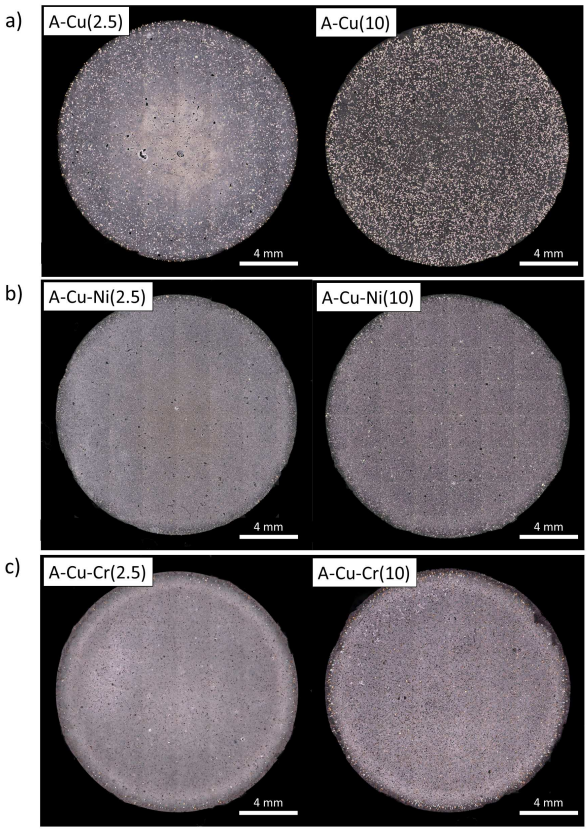

Figure 3. Photographs of the sample surfaces of the systems: a) Al_2O_3-Cu, b) Al_2O_3-Cu-Ni and c) Al_2O_3-Cu-Cr

level of 96–97 %TD. Due to the high density of the samples, the porosity and absorbability of the obtained composites was <1%. Based on the measurements, it was found that the volumetric shrinkage of the composites ranged from 37% to 40%. The highest volumetric shrinkage was recorded for the samples from series A-Cu(2.5) and A-Cu-Cr(2.5). The tests showed that the obtained samples were characterized by linear shrinkage determined on the diameter in the range from 14% to 16%, and on the height of the sample in the range from 13% to 15%. The obtained results for selected physical properties are summarized in Table 2.

Phase composition analysis of the sintered Al_2O_3-Cu and Al_2O_3-Cu-Cr composites (Fig. 4) did not show the presence of new phases in the structure. In the Al_2O_3-Cu composites, peaks from alumina (PDF #04-014-1368) and copper (PDF #04-013-9963) were found. The composites of the Al_2O_3-Cu-Cr system, apart from aluminium oxide (PDF #98-00-0174) and copper (PDF #04-013-9963) were characterized by the presence of Cr reflections in the diffractograms (PDF #04-004-8454). In the case of Al_2O_3-Cu-Ni composites, the analysis of the diffraction patterns obtained for both manufactured series showed reflections from Al_2O_3 (PDF #04-015-8994), Cu (PDF #04-002-8504), Ni (PDF #04-003-7263) and CuNi solid solution (PDF #01-071-7832). The presence of the latter confirms the formation of a new phase during the sintering process resulting from the reaction between the nickel particles and liquid copper. With the increase of metallic phase content in the sample, the probability of contact between Ni and Co particles increases during sintering, and thus the proportion of the new phase in the sintered sample raises.

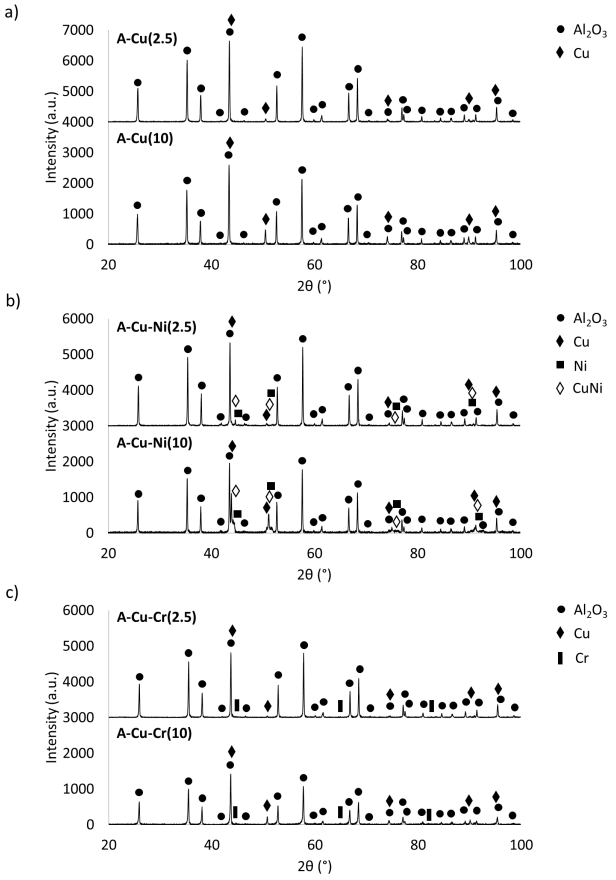

Figure 4. Diffractograms of sintered composites: a) Al_2O_3-Cu, b) Al_2O_3-Cu-Ni and c) Al_2O_3-Cu-Cr

Table 2. Selected physical properties of the sintered samples

Sample	Theoretical density [g/cm^3]	Relative density [%TD]	Open porosity [%]	Water absorption [%]	Volumetric shrinkage [%]	Linear diameter shrinkage [%]	Height shrinkage [%]
A-Cu(2.5)	4.11	96.99 ± 0.38	0.110 ± 0.083	0.028 ± 0.021	40.91 ± 0.74	16.34 ± 0.09	15.56 ± 0.90
A-Cu(10)	4.49	97.32 ± 0.11	0.152 ± 0.052	0.035 ± 0.012	37.68 ± 0.73	15.24 ± 0.03	13.27 ± 1.06
A-Cu-Ni(2.5)	4.11	97.21 ± 0.03	0.045 ± 0.004	0.011 ± 0.001	39.54 ± 0.62	16.48 ± 0.06	13.32 ± 0.86
A-Cu-Ni(10)	4.48	97.09 ± 0.11	0.233 ± 0.039	0.054 ± 0.009	37.04 ± 0.44	14.87 ± 0.07	13.13 ± 0.62
A-Cu-Cr(2.5)	4.09	97.79 ± 0.15	0.091 ± 0.025	0.023 ± 0.006	40.45 ± 0.32	16.43 ± 0.07	14.73 ± 0.28
A-Cu-Cr(10)	4.40	96.58 ± 0.53	0.523 ± 0.293	0.123 ± 0.070	38.90 ± 0.34	15.23 ± 0.18	14.98 ± 0.52

Hence, higher intensity of the peaks coming from the CuNi solution is clearly visible in the diffraction pattern of A-Cu-Ni(10) sample. The obtained results are confirmed by previous studies published by our team on composites from the Al_2O_3-Cu-Ni system, where the phase composition analysis also confirmed the formation of a CuNi solid solution after the sintering process [28].

In the Al_2O_3-Cu samples (Fig. 4a), reflections corresponding to the following Cu crystallographic planes were observed: (111), (200), (220), (311) and (222). For the A-Cu(2.5) and A-Cu(10) composites, the reflections from the defined planes occurred at 2θ of 43.47°, 50.50°, 74.12°, 89.96°, 95.28° and 43.41°, 50.45°, 74.12°, 89.88°, 95.25°, respectively.

In the case of samples from the Al_2O_3-Cu-Ni system (Fig. 4b), reflections corresponding to the families of Cu planes: (111), (200), (220), (311) and (222) were observed. For the A-Cu-Ni(2.5) and A-Cu-Ni(10) composites, the reflections from the defined planes occurred at 2θ of 43.87°, 50.70°, 74.45°, 90.86° and 95.15° and 43.67°, 51.10°, 74.99°, 91.25°, 96.48°, respectively. In addition, reflections corresponding to Ni planes: (111), (200), (220) and (311) were also observed at 2θ angle of 45.33°, 51.96°, 76.32°, 91.59° and 44.36°, 51.77°, 76.28°, 92.72° for the A-Cu-Ni(2.5) and A-Cu-Ni(10), respectively. In the XRD patterns of the A-Cu-Ni(2.5) and A-Cu-Ni(10) samples, the presence of four reflections, corresponding to (111), (200), (220) and (311) planes, was also revealed, which should be attributed to the CuNi solid solution. For the A-Cu-Ni(2.5) and A-Cu-Ni(10) samples at the 2θ angle values for different planes are equal to: 44.37°, 51.73°, 75.67°, 91,94° and 44.21°, 51.60°, 75.90°, 92.28°, respectively.

The analysis for the samples from the Al_2O_3-Cu-Cr system (Fig. 4c) showed, as in the case of samples of the Al_2O_3-Cu reference series, the presence of reflections corresponding to the following Cu crystallographic planes: (111), (200), (220), (311) and (222). For the A-Cu-Cr(2.5) and A-Cu-Cr(10) composites, the reflections from the defined planes occurred at 2θ of 43.49°, 50.52°, 74.11°, 89.91°, 95.24° and 43.65°, 50.73°, 74.33°, 90.05°, 95.34°, respectively. In addition, the presence of reflections corresponding to the families of Cr crystallographic planes: (110), (200) and (211) was confirmed in the analysed samples. For the A-Cu-Cr(2.5) sample, successive planes were observed at the 2θ angle of: 44.48°, 64.70°, 82.38°, while for the A-Cu-Cr(10) sample, at the 2θ angle of: 44.66°, 65.27°, 81.97°.

In the next stage of the research, the produced samples were subjected to monotonic compression. The strain diagram of the samples due to monotonic compression is shown in Fig. 5. On the other hand, Fig. 6 presents a summary of the deformation distribution using the digital image correlation method for one exemplar sample from the tested series.

Based on the obtained results, it was found that the A-Cu(2.5) samples withstood a load of 13 kN and had

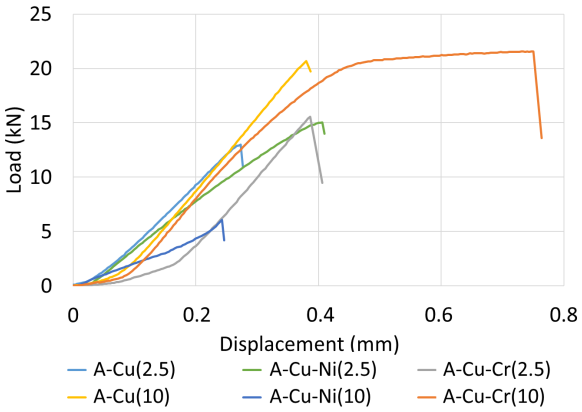

Figure 5. Dependence of the destructive force on the strain

a displacement of 0.27 mm. The distribution of deformations during compression was uniform throughout the sample area, except for the contact zones with the loading platform. The resulting deformation resulted in an even stress distribution along the load axis (Fig. 6b, A-Cu(2.5)). The crack occurred at a distance of about 5 mm along the load axis of the sample. The cracking process was multifaceted (Fig. 6c, A-Cu(2.5)). This proves to be disordered, but even distribution of the materials included in the sample.

The tests showed that the A-Cu(10) sample was characterized by a load of 15 kN. The crushing of the samples to the moment of failure was 0.41 mm. The strain distribution at the moment of maximum load showed local displacements of the sample structure over its entire surface (Fig. 6b, A-Cu(10)). Despite the significant deformation of the sample, the cracking occurred along the load axis (Fig. 6c, A-Cu(10)).

The A-Cu-Ni(2.5) sample carried a load of 15.6 kN. The crushing of the samples to the moment of destruction was 0.38 mm. The samples maintained a uniform distribution of deformations during loading (Fig. 6b, A-Cu-Ni(2.5)). Upon reaching the critical load, the sample was dynamically fragmented into numerous fragments (Fig. 6c, A-Cu-Ni(2.5)).

Monotonic compression tests showed that the A-Cu-Ni(10) sample withstood a load of 20.6 kN and a displacement of 0.38 mm. The distribution of deformations during compression was uniform in the entire area of the samples with a noticeable intensification in the loading axis zone. The resulting deformation resulted in an even stress distribution along the load axis (Fig. 6b, A-Cu-Ni(10)). The crack occurred at a distance of about 5 mm along the load axis of the sample. The course of the cracking process was single-plane (Fig. 6c, A-Cu-Ni(10)). This proves to be ordered and even distribution of the materials included in the sample.

The A-Cu-Cr(2.5) sample withstood a load of 6.5 kN and a displacement of 0.24 mm. The strain distribution at the moment of maximum load showed a crack along the load axis of the sample (Fig. 6b, A-Cu-Cr(2.5)). The cracking occurred along the axis of the sample (Fig. 6c, A-Cu-Cr(2.5)).

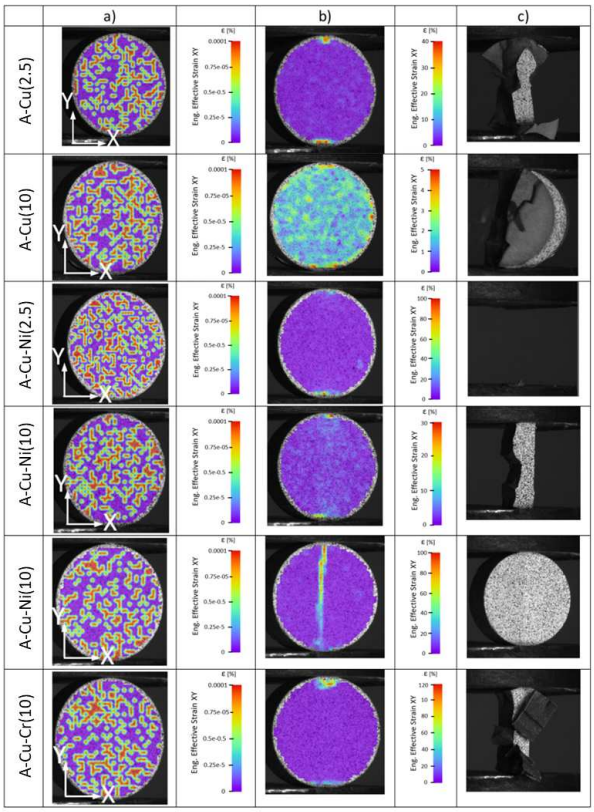

Figure 6. Distribution of strains using the digital image correlation method: a) reference state, b) maximum strain state and c) cracking course

In the case of the A-Cu-Cr(10) sample, the composite withstood a load of 21.5 kN and a displacement of 0.75 mm. The distribution of deformations during compression concentrated in the upper area at the point of contact between the sample and the loading platform. The resulting deformation resulted in an even stress distribution along the load axis (Fig. 6b, A-Cu-Cr(10)). The crack occurred at a distance of about 5 mm along the load axis of the sample. The course of the cracking process was single-plane (Fig. 6c, A-Cu-Cr(10)). This proves to be ordered and even distribution of the materials included in the sample.

Figures 7-9 show SEM micrographs of the prepared samples. The micrographs were compiled for the samples from the same system, but differing in the content of the metallic phase in the structure.

The analysis of breakthroughs for the samples from the Al_2O_3-Cu system (Fig. 7) revealed poor adhesion at the interface between the ceramic matrix and the metal. The cracks, choosing the propagation path with the lowest energy, ran at the contact point of the components. This is also illustrated by the surface of the metallic particles present in the structure with a visible representation of the matrix grains detached during cracking. At the contact boundary between the components, the presence of stratifications was also observed, confirming poor adhesion between the components. The main reason is the low wettability between Al_2O_3 and Cu (con-

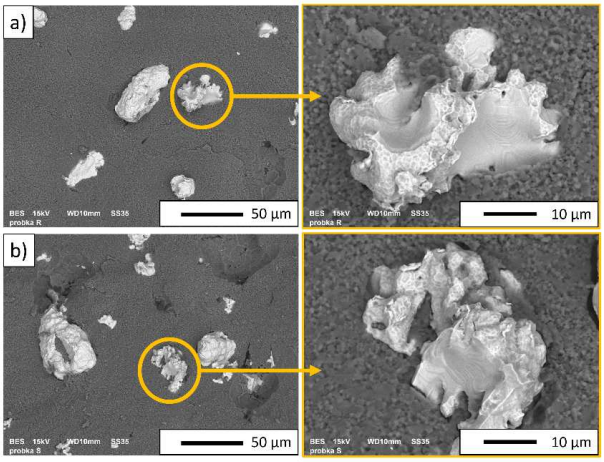

Figure 7. Breakthroughs of samples from the Al_2O_3-Cu system: a) 2.5 and b) 10 vol.% of the metallic phase

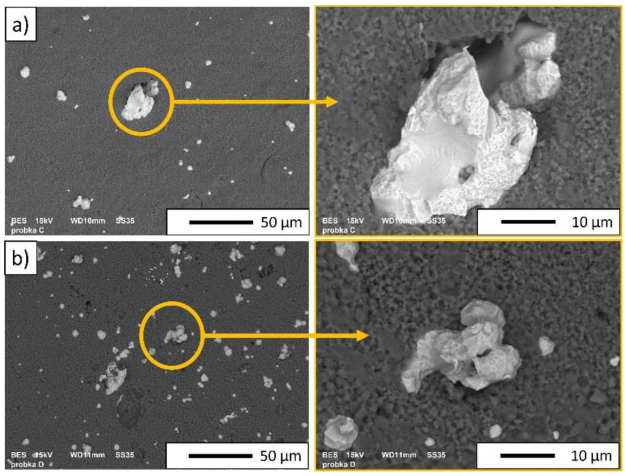

Figure 8. Breakthroughs of samples from the Al_2O_3-Cu-Ni system: a) 2.5 and b) 10 vol.% of the metallic phase

tact angle >90°). The matrix particles were characterized by a morphology similar to that of the starting powder. The copper particles were characterized by high irregularity, not maintaining the dendritic character of the starting powder. The low melting point of Cu causes that during the sintering process, the metallic phase composed of copper remains in a liquid state and takes the form in which it is closed by the ceramic matrix particles growing during the sintering process. In the case of the samples with a higher content of the metallic phase, the probability of contact between metallic particles was higher, so the presence of metallic areas in the structure was observed as a result of the connection of several copper particles during sintering.

Observations of fractures of the samples with Ni (Fig. 8) also revealed the presence of metallic particles of irregular structure. In the case of a higher content of the metallic phase, areas where the particles merged into clusters as a result of contact during sintering were visible. The metal-matrix contact boundary was characterized by a slightly smaller number of stratifications, which may suggest the influence of nickel on the im-

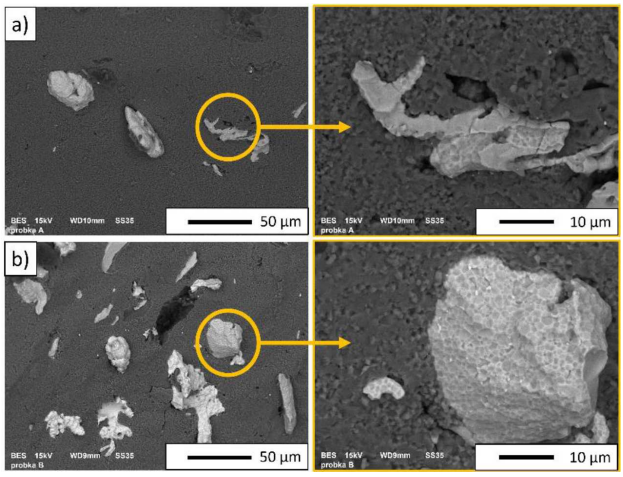

Figure 9. Breakthroughs of samples from the Al_2O_3-Cu-Cr system: a) 2.5 and b) 10 vol.% of the metallic phase

provement of adhesion between the components. However, the fracture process of the material continued at the interface of the components, suggesting that the improvement, if any, had no significant effect on the nature of the fracture or the course of the fracture process during its formation. There is also an increase in the size of Al_2O_3 particles in the structure with the increase in the proportion of the metallic phase. However, the morphology of the matrix particles remained unchanged.

In the case of the samples with Cr (Fig. 9), the occurrence of irregular metallic particles in the fracture structure was also observed. There were no stratifications at the component boundary, but there are visible losses caused by tearing out of metallic particles during the cracking process. It is worth noting, however, that in addition to cracking at the interface of the components in the samples, crack planes within the metallic particles themselves are also visible. This may be related to the presence of Cr, a metal with much lower plasticity than Cu and Ni, the presence of which may improve mechanical properties. It also suggests the possibility of areas in the sample with improved adhesion at the interface of the components.

Based on the SEM image with higher magnification (Fig. 10.), histograms showing the distribution of alumina grains for individual series were obtained. Figures 11-13 present the results of the image analyses in the form of histograms of grain size distribution (the equivalent diameter d_2 of the matrix grains). In the case of the samples from the Al_2O_3-Cu system (Fig. 11), the histograms are characterized by a similar, unimodal distribution with a clearly visible peak corresponding to the most common grain fraction. For the samples with a lower content of the metallic phase, this peak is in the range of 0.6–0.8 µm. With the increase in the content of the metallic phase, a slight shift in the range of maxi-

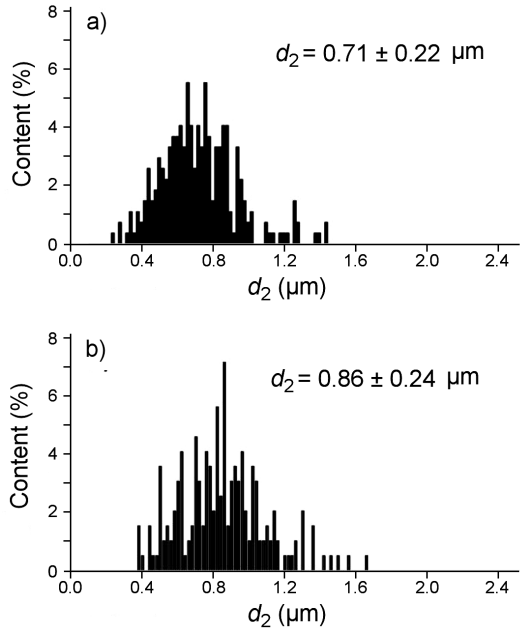

Figure 11. Histogram of the percentage distribution of the d_2 diameter value for samples from the Al_2O_3-Cu system: a) 2.5 and b) 10 vol.% of the metallic phase

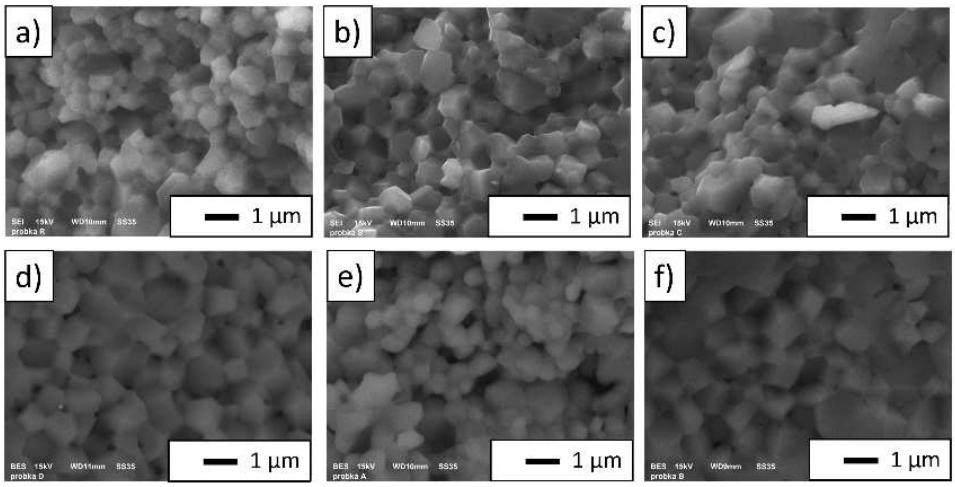

Figure 10. SEM micrographs of samples: a) A-Cu(2.5), b) A-Cu(10), c) A-Cu-Ni(2.5), d) A-Cu-Ni(10), e) A-Cu-Cr(2.5) and f) A-Cu-Cr(10)

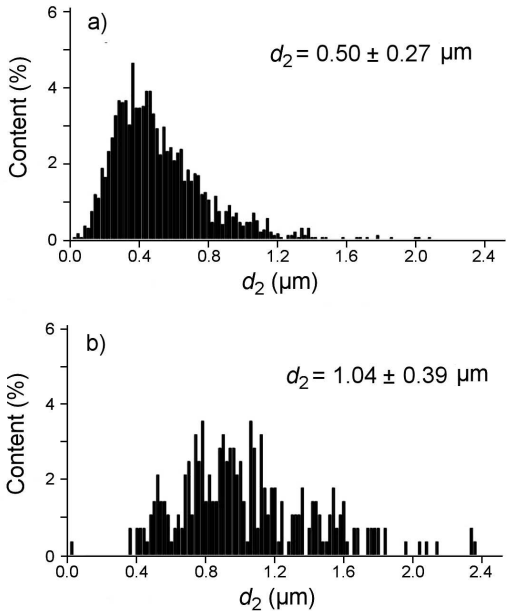

Figure 12. Histogram of the percentage distribution of the d_2 diameter value for samples from the Al_2O_3-Cu-Ni system: a) 2.5 and b) 10 vol.% of the metallic phase

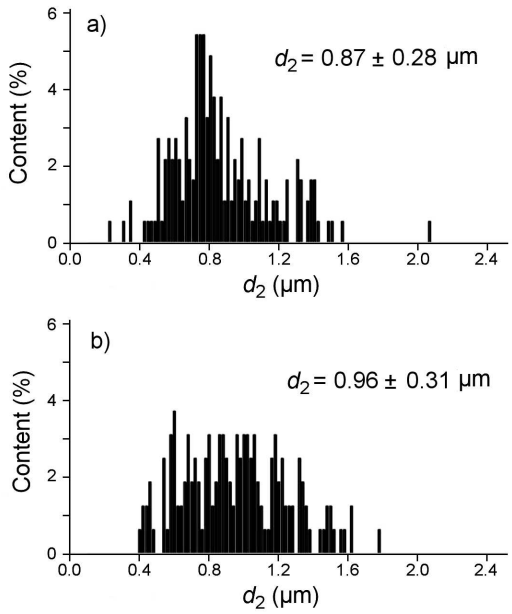

Figure 13. Histogram of the percentage distribution of the d_2 diameter value for samples from the Al_2O_3-Cu-Cr system: a) 2.5 and b) 10 vol.% of the metallic phase

mum values was observed towards larger d_2 values in the range of 0.7–0.9 μm.

An analogous relationship was observed in the case of the samples from ternary systems. Replacement of Cu partially with Ni resulted in shifting the d_2 range towards lower values for the sample with 2.5 vol.% of metallic phase (range of d_2 is 0.2–0.5 μm). However, increasing the proportion of the metallic phase in the sample to 10 vol.% resulted in shifting the range of the most common d_2 values to d_2 = 0.8–1.2 μm. Thus, the presence of lower component of metallic phase in the A-Cu-Ni(10) inhibited the growth of the matrix grains, but the higher amount of metallic phase is not efficient.

In the case of the Al_2O_3-Cu-Cr sample with 2.5 vol.% of the metallic phase content, similar results were obtained as in the reference sample with Cu. The histogram is unimodal with d_2 values in the range of d_2 = 0.7–0.9 μm. The increase in content of the metallic phase in the composite to 10 vol.% caused the growth of Al_2O_3 grains. The histogram in this case is characterized by the occurrence of a wide range of equivalent diameter values without a clear maximum with d_2 in the range 0.6–1.2 μm.

It can be concluded that the increase in the proportion of the metallic phase led to an increase in the diameter d_2 of the Al_2O_3 matrix grains. The largest difference was observed for the samples with nickel, while the smallest changes were observed in the case of the reference samples from the Al_2O_3-Cu system.

In the next step, the stereological analysis was used to evaluate shape parameters for Al_2O_3 grains in individual series and obtained results are presented in Table 3. The stereological analysis showed that, regardless of the tested series, the alumina grains are characterized by a similar shape. It was also found that all composites are characterized by oval, slightly elongated shapes. In addition, based on the obtained results, no effect of the addition of the third metallic component on the shape of aluminium oxide grains in the prepared samples was found.

IV. Conclusions

The article analyses the possibility of producing composites based on Al_2O_3 matrix with copper. We tried to determine how the structure and mechanical properties are affected by replacing part of Cu with a second metallic component (Ni or Cr). Using uniaxial pressing with pressure-less sintering, six samples were produced from three systems: Al_2O_3-Cu, Al_2O_3-Cu-Ni and Al_2O_3-Cu-

Table 3. Average values of shape parameters for Al_2O_3 grains of sintered samples

Sample	Shape factors for Al_2O_3 grains		
	Curvature of grain boundary, R	Elongation, α	Convexity, W
A-Cu(2.5)	1.16 ± 0.01	1.26 ± 0.02	1.08 ± 0.01
A-Cu(10)	1.15 ± 0.01	1.29 ± 0.02	1.08 ± 0.01
A-Cu-Ni(2.5)	1.25 ± 0.01	1.38 ± 0.02	1.08 ± 0.01
A-Cu-Ni(10)	1.13 ± 0.06	1.31 ± 0.04	1.09 ± 0.02
A-Cu-Cr(2.5)	1.16 ± 0.05	1.32 ± 0.04	1.10 ± 0.01
A-Cu-Cr(10)	1.20 ± 0.06	1.33 ± 0.04	1.10 ± 0.02

Cr with a 2.5 and 10 vol.% of the metallic phase content.

Possibility of producing composite samples with satisfactory density was confirmed and for all series it exceeded 95 %TD. However, no significant influence of the composition on the obtained density values was found. The phase composition analysis confirmed that there is no secondary phase except in the case of the Al_2O_3-Cu-Ni samples, where a new phase is formed during sintering (CuNi solid solution). The microstructure observations showed that the addition of the second metallic component has a positive effect on the size and distribution of the metallic particles, limiting the formation of metal clusters. Partial replacement of Cu with Ni resulted in the decrease of Al_2O_3 grain size for the sample with 2.5 vol.% of metallic phase. However, irrespective of the system, a higher content of the metallic phase led to an increase in the size of the Al_2O_3 grains. The largest increase was noted for nickel samples, and the smallest was observed between series of chromium samples.

Compressive strength tests have shown that the addition of the second metallic phase has a positive effect on the compressive strength of the composites. While the samples with copper withstood a similar load, regardless of the proportion of the metallic phase, in the samples from the ternary systems, the compressive strength increased with the increase in the proportion of the metallic phase. Observations of the fracture surface confirmed the poor adhesion between the ceramic matrix and the metallic phase. The main plane of cracking of the material was the phase boundary between the matrix and the metallic particles.

Acknowledgements: The study was accomplished thanks to the funds allotted by The National Science Centre within the framework of the research project 'OPUS 13' No. 2017/25/B/ST8/02036.

References

1. M. Barsoum, *Fundamentals of Ceramics*, CRC Press, 2019.
2. N. Travitzky, "Processing of ceramic-metal composites", *Adv. Appl. Ceram.*, **111** (2011) 286–300.
3. A.J. Ruys, *Alumina Ceramics: Biomedical and Clinical Applications*, Woodhead Publishing, 2018.
4. C.B. Carter, M.G. Norton, *Ceramic Materials: Science and Engineering*, Springer, New York, NY, 2013.
5. E. Rocha-Rangel, J. López-Hernández, C.A. Calles-Arriaga, W.J. Pech-Rodríguez, E.N. Armendáriz-Mireles, J.A. Castillo-Robles, J.A. Rodríguez-García, "Effect of additions of metal submicron particles on properties of alumina matrix composites", *J. Mater. Res.*, **34** (2019) 2983–2989.
6. J.A. Yeomans, "Ductile particle ceramic matrix composites - Scientific curiosities or engineering materials?", *J. Eur. Ceram. Soc.*, **28** (2008) 1543–1550.
7. D.M. Liu, W.H. Tuan, "Microstructure and thermal conduction properties of Al_2O_3 Ag composites", *Acta Mater.*, **44** (1996) 813-818.
8. S. Shi, S. Cho, T. Goto, T. Sekino, "The effects of sintering temperature on mechanical and electrical properties of Al_2O_3/Ti composites", *Mater. Today Commun.,* **25** (2020) 101522.
9. H.M. Irshad, A.S. Hakeem, B.A. Ahmed, Sh. Ali, S. Ali, S. Ali, M.A. Ehsan, T. Laoui, "Effect of Ni content and Al_2O_3 particle size on the thermal and mechanical properties of Al_2O_3/Ni composites prepared by spark plasma sintering", *Int. J. Refract. Hard Met.*, **76** (2018) 25–32.
10. J.G. Song, Y. Liu, C.X. Wu, "Fabrication and properties of Al_2O_3-Al cermet materials using different raw material composition parameter", *J. Ceram. Process. Res.,* **21** (2020) 21–25.
11. D. Zhang, C. Chu, S. Ma, Y. Wang, C. Duan, J. Guo, X. Shi, G. Xu, Y. Cheng, A. Sun, "A novel method to avoid the sintering shrinkage of Al_2O_3-Cr cermets formed by direct ink writing", *J. Alloys Compd.,* **931** (2023)167632.
12. J.R. Davis, *Copper and Copper Alloys*, ASM International, 2001.
13. J.A. Cahill, A.D. Kirshenbaum, "The density of liquid copper from its melting point (1356 °K) to 2500 °K and an estimate of its critical constants", *J. Phys. Chem.* **66** (1962) 1080–1082.
14. P.D. Ownby, J. Liu, "Surface energy of liquid copper and single-crystal sapphire and the wetting behavior of copper on sapphire", *J. Adhes. Sci. Technol.*, **2** (1988) 255–269.
15. S-T. Oh, J.S. Lee, T. Sekino, K. Niihara, "Fabrication of Cu dispersed Al_2O_3 nanocomposites using Al_2O_3/CuO and Al_2O_3/Cu-nitrate mixtures", *Scr. Mater.*, **44** (2001) 2117–2120.
16. T. Feng, W. Zheng, W. Chen, Y. Shi, Y.Q. Fu, "Enhanced interfacial wettability and mechanical properties of Ni@Al_2O_3/Cu ceramic matrix composites using spark plasma sintering of Ni coated Al_2O_3 powders", *Vacuum*, **184** (2021) 109938.
17. N.A. Travitzky, "Microstructure and mechanical properties of alumina/copper composites fabricated by different infiltration techniques", *Mater. Lett.*, **36** (1998) 114–117.
18. K. Sang, Y. Weng, Z. Huang, X. Hui, H. Li, "Preparation of interpenetrating alumina-copper composites", *Ceram. Int.*, **42** (2016) 6129–6135.
19. K. Jach, K. Pietrzak, A. Wajler, A. Strojny-Nedza, "Fabrication of an alumina-copper composite using a ceramic preform", *Powder. Metall. Met. Ceram.*, **52** (2014) 680–685.
20. S.T. Oh, K.M. Kang, "Effect of sintering atmosphere on the microstructure of hot-pressed Al_2O_3/Cu nanocomposites", *Mater. Sci. Forum*, **449-452** (2004) 1217–1220.
21. J. Zhang, T. Goto, "Fabrication of Al_2O_3-Cu nanocomposites using rotary chemical vapor deposition and spark plasma sintering", *J. Nanomater.*, **4** (2015) 4.
22. Y. Shi, W. Chen, L. Dong, H. Li, Y. Fu, "Enhancing copper infiltration into alumina using spark plasma sintering to achieve high performance Al_2O_3/Cu composites", *Ceram. Int.*, **44** (2018) 57–64.
23. K.H. Min, S-T. Oh, Y.D. Kim, I.H. Moon, "Processing and fracture toughness of nano-sized Cu-dispersed Al_2O_3 composites", *J. Alloys Compd.*, **352** (2003) 163–167.
24. J. Miranda-Hernández, S. Moreno-Guerrero, A.B. Soto-Guzmán, E. Rocha-Rangel, "Production and characterization of Al_2O_3-Cu composite materials", *J. Ceram. Process. Res.*, **7** (2006) 311–314.
25. E. Rocha-Rangel, J.G. Miranda-Hernández, "Alumina-

copper composites with high fracture toughness and low electrical resistance", *MSF*, **644** (2010) 43–46.
26. M. Stratigaki, W. Pabst, V. Nečina, M. Hajíček, A.D. Gotsis, "Microstructure and mechanical properties study of slip-cast copper-alumina composites", *SN Appl. Sci.*, **1** (2018) 40.
27. P. Piotrkiewicz, J. Zygmuntowicz, A. Miazga, J. Szymańska, M. Wachowski, W. Kaszuwara, "The influence of metal phase composition on microstructure and mechanical properties of Al_2O_3-Cu-Cr ceramic metal composites", *Process. Appl. Ceram.*, **14** (2020) 251–259.
28. J. Zygmuntowicz, B. Bulski, J. Szymańska, P. Piotrkiewicz, W. Kaszuwara, "Characterization of the alumina oxide, copper and nickel powders and their processing intended for fabrication of the novel hybrid composite: A comparative study", *Materialwiss. Werksttech.*, **52** (2021) 379–391.
29. P. Piotrkiewicz, J. Zygmuntowicz, M. Wachowski, K. Cymerman, W. Kaszuwara, A. Więcław Midor, "Al_2O_3-Cu-Ni composites manufactured via uniaxial pressing: Microstructure, magnetic, and mechanical properties", *Materials*, **15** (2022) 1848.
30. J. Zygmuntowicz, P. Falkowski, M. Wachowski, K. Cymerman, P. Piotrkiewicz, W. Kaszuwara, "Effect of the sintering temperature on microstructure and properties of Al_2O_3–Cu–Ni hybrid composites obtained by PPS", *Int. J. Appl. Ceram. Technol.*, **17** (2020) 1731–1741.
31. T. Massalski, H. Okamoto, *Binary Alloy Phase Diagrams*, ASM International: Materials Park, OH USA, 1990.
32. J. Schmitz, J. Brillo, I. Egry, "Surface tension of liquid Cu and anisotropy of its wetting of sapphire", *J. Mater. Sci.*, **45** (2010) 2144–2149.
33. E. Gorges, I. Egry, "The surface tension of copper-nickel alloys", *J. Mater. Sci.*, **30** (1995) 2517–2520.